AR-010-105

DSTO-TR-0477

Effectiveness of High Modulus Interference-Fit Bushes for Fatigue Life Extension of Plates with Circular Holes

Rebecca Evans

DISTRIBUTION STATEMENT A
Approved for public release
Distribution Unlimited

APPROVED FOR PUBLIC RELEASE

19970624 093

DEPARTMENT ◆ OF DEFENCE

DEFENCE SCIENCE AND TECHNOLOGY ORGANISATION

Effectiveness of High Modulus Interference-Fit Bushes for Fatigue Life Extension of Plates with Circular Holes

Rebecca Evans

Airframes and Engines Division
Aeronautical and Maritime Research Laboratory

DSTO-TR-0477

ABSTRACT

An experimental program has been carried out to examine the influence of bush modulus on the fatigue lives of aluminium alloy specimens with bushed holes of 12 mm diameter. The specimens, with 1 mm or 2 mm thick bushes of 0.5% interference fit and of widely different modulus, were fatigue tested under a representative fighter-aircraft loading sequence. The thin-walled bushes were found to extend the fatigue lives of the plates with holes by at least 4.2 times, and the thick-walled bushes produced at least a 10.9 times increase in life. The test results also indicated that different failure modes can occur depending on the relative thickness and modulus of the interference-fit bush. Thus, the specimens with the highest bush modulus did not necessarily have the longest lives, even though the stress concentration factor (due to remote loading) at the hole edge for these specimens was the lowest. Finite-element work was also conducted to determine the stresses and strains in the interference-fit bushes for conditions of no-slip and frictionless contact between the bush and plate. High tensile strains were found to occur in the bush at the inner surface.

RELEASE LIMITATION

Approved for public release

DEPARTMENT OF DEFENCE

DEFENCE SCIENCE AND TECHNOLOGY ORGANISATION

Published by

DSTO Aeronautical and Maritime Research Laboratory
PO Box 4331
Melbourne Victoria 3001

Telephone: (03) 9626 8111
Fax: (03) 9626 8999

AR No. 010-105
February 1997

APPROVED FOR PUBLIC RELEASE

Effectiveness of High Modulus Interference-Fit Bushes for Fatigue Life Extension of Plates with Circular Holes

Executive Summary

Holes exist in metallic aircraft structures for either design or construction reasons and their stress concentrating effect is such that they are common regions of crack initiation. Theoretical and experimental investigations have respectively predicted and confirmed that the fatigue life of a plate with a hole can be increased by the use of an interference-fit insert. Some theoretical studies have considered inserts of various materials and wall thickness. However, very limited experimental verification has been given in the literature to assess the potential benefit of using various materials and wall thickness for the inserts.

A testing program to experimentally investigate the effect of the modulus of an interference-fit bush on the fatigue life of an aluminium plate with a central hole has been carried out at AMRL. This report presents the results of the study which examined specimens with 1 mm or 2 mm thick bushes of 0.5% interference fit and of different materials; namely aluminium, steel and tungsten carbide. The specimens were fatigue tested under a representative fighter-aircraft loading sequence. The thin-walled bushes extended the fatigue lives of the plates with holes by at least 4.2 times, and the thick-walled bushes produced at least a 10.9 times increase in life. The test results also indicated that different failure modes can occur depending on the relative thickness and modulus of the interference-fit bush. The specimens with the highest bush modulus did not necessarily have the longest lives, even though the stress concentration factor (due to remote loading) at the hole edge for these specimens was the lowest. Finite-element work was also conducted to determine the stresses and strains in the interference-fit bushes for conditions of no-slip and frictionless contact between the bush and plate. High tensile strains were found to occur in the bush at the inner surface.

It has been experimentally demonstrated that interference-fit bushes of various modulus offer a potential life extension option for plates containing open holes, such as those occurring in RAAF aircraft components.

Authors

Rebecca Evans
Airframes and Engines Division

Rebecca Evans completed a Bachelor of Engineering in Aeronautical Engineering at the Royal Melbourne Institute of Technology in 1987. In 1988 she commenced work in Systems Division at DSTO Salisbury, where she worked on the design, analysis and testing of towed targets. Since 1992 she has been working in the Airframes and Engines Division where she has undertaken experimental and finite-element analyses of metallic aircraft components, evaluating various fatigue life enhancement techniques.

Contents

1. Introduction

Considerable theoretical and experimental work has been completed to investigate the effect of interference-fit bushes on the fatigue life of plates with holes. A few papers have discussed the added variable of the material of the bush [Refs. 1-4]. These studies indicate that under remote loading more load is transferred from the plate to the interference-fit bush with increasing bush modulus, hence resulting in a greater reduction in maximum alternating stress in the plate at the hole edge.

Finite-element methods were used by Piperias and Heller [1] to determine stresses in a uniaxially loaded finite plate, with an interference-fit bush or bush/bolt combination. By varying the bush modulus and thickness, the alternating and interference stresses in the plate were altered. Koplik and Klassen [2], determined the stress and displacement distributions of an infinite plate/interference-fit insert system using Airy stress functions. Values of friction coefficient were calculated which ensured the condition of no-slip between the plate and insert (of various moduli). Stresses in an infinite uniaxially-loaded plate with an interference-fit bolt were analytically calculated for no-slip and frictionless contact between the plate and the bolt, by Crews in [3]. Stress distributions in the plate were determined for various combinations of plate and bolt moduli. Results include hoop and radial stresses around the hole boundary and plate transverse axis, for interference only and total load. In [4], elastic and plastic stress and strain distributions were determined for an elastic/perfectly plastic annulus which had remote (radial) loading, interference loading, or a combination of the two.

There is a lack of experimental verification in the literature to assess the potential of using various materials and wall thickness for the bushes. There is also limited information available on the interference and alternating stresses in interference-fit bushes in finite-width plates. Thus, this report describes such a testing program conducted at AMRL, and presents results from finite-element analysis of the stresses in interference-fit bushes.

Aluminium plates with bushes of 0.5% interference-fit and 1 mm or 2 mm wall thickness were fatigue tested under a fighter-aircraft loading sequence. The bushes were of three different materials; namely aluminium, steel or tungsten-carbide; the ratio of bush to plate modulus being equal to 1.0, 2.9 and 7.5, respectively. Specimens without bushes were also tested for reference. Preliminary tests were also undertaken with similar specimens which had steel or ceramic interference-fit bushes of 2 mm wall thickness. The outcomes of this preliminary work included the following; surface treatments were necessary to reduce the probability of failure from the fillets, the ceramic bushes could not withstand the insertion loads and the use of barium chromate as an insertion aid did not appear to affect the fatigue life of the specimens.

On account of the failure of the ceramic bushes in the preliminary tests and due to the lack of useable data from previous studies, finite-element modelling was completed to

determine interference and alternating stresses in the bushes, for no-slip and frictionless (slip) contact on the plate/bush interface. For the test loads applied, a combination of these two conditions occurs. Even though [2] addresses stresses in the bush, the assumption of no-slip restricted the use of the equations. Due to the no-slip assumption, the material, geometry and interference level of the bushes resulted in an unrealistic, very large calculated value of friction coefficient and small value of applied stress.

A description of the finite-element numerical analysis is given in Section 2. This is followed in Sections 3 and 4 with specimen details, and testing details and results for the thick and thin bushed specimens respectively.

2. Numerical Analysis

The preliminary specimens which were tested with ceramic (pollycrystalline alumina) bushes were unsatisfactory. The bushes cracked circumferentially when inserted into the plate due to the complex three-dimensional stress field produced in the bush on insertion. When the specimens were fatigue tested, the bushes rapidly crumbled under the applied loading, resulting in the testing of only plates with a hole. Alumina has a Young's modulus (E) of 390 MPa, over five times that of the aluminium alloy of the plates, however, its tensile strength is very low. It was thus decided to complete a finite-element (FE) analysis to determine typical stresses and strains in interference-fit bushes of different materials. As a consequence the required material properties were determined, and tungsten-carbide H15F was selected for the highest modulus bush material and was used in all subsequent testing ($E_{bush}/E_{plate} \geq 7$).

In addition to this, limited results have been presented in the literature in useable form for the magnitude of stresses in the insert. This is partly due to the fact that the primary focus of work has been on the effect of alternating stresses in the reinforced plate. In this section the results of FE analyses are given for various moduli of inserts, for the geometry case investigated experimentally in Section 3.

2.1 Method

In this FE work, the general geometry under consideration is a rectangular plate, with an interference-fit bush, loaded remotely with a uniaxial stress as shown in Figure 1. Two-dimensional elastic plane-stress models, for the conditions of no-slip and slip between the plate and the bush, were studied as two bounds to the real solution. In practice the no-slip solution would be valid up until a particular remote loading, depending on the magnitude of shear stress, normal force and friction coefficient at a location around the boundary. As the remote load is increased, slip would then occur locally; the region(s) of slip increasing with increase in load.

The finite-element models used were modified versions of the rectangular plate model given by Allan and Heller [5]. The interference modelling method is valid providing there is no separation between the bush and plate. Due to symmetry, only one quarter of the structure was modelled (as shown in Fig. 2). For all analyses the half height and half width of the plate was 75 mm and 150 mm respectively, and the hole radius 10 mm. The plate material was aluminium alloy with a Young's modulus (E) of 72.4 GPa and Poisson's ratio (ν) of 0.33, and the interference-fit bush and plate were 5 mm in thickness. Analyses were undertaken using the PAFEC (Program for Automatic Finite Element Calculations) suite of programs, level 8.1, run on a HP9000-755 computer. Displacement constraint equations between the bush and plate interface nodes were used to model the interference-fit conditions of no-slip and slip for all pairs of nodes around the boundary. The schematic of Figure 3 depicts two adjacent nodal points on the bush and the plate boundaries prior to bush insertion. The two points become coincident following the insertion of the bush. For the no-slip case these nodes were linked radially and hoopwise to satisfy the two boundary conditions on insertion of the oversize bush into the hole;

$$u_{\text{plate}} - u_{\text{bush}} = \delta$$
$$v_{\text{plate}} - v_{\text{bush}} = 0$$

where δ = difference in initial bush and hole radii.

For the slip case, these nodes were linked radially only, ie, no tangential constraint, to satisfy the interference-fit boundary condition.

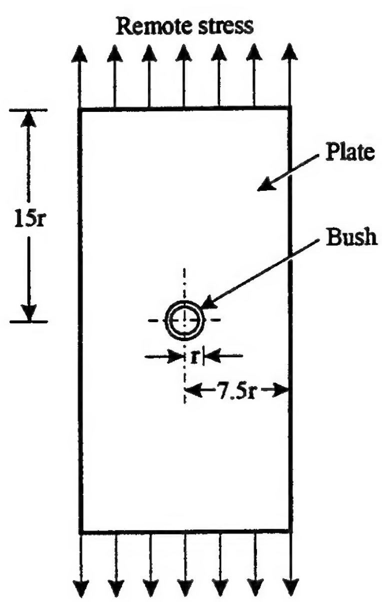

Figure 1. Geometry for interference-fit bush models

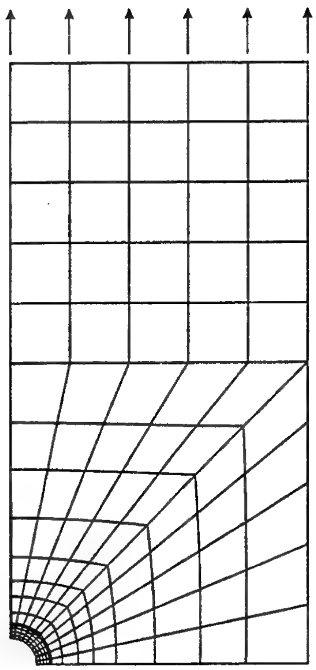

(a) Overall model

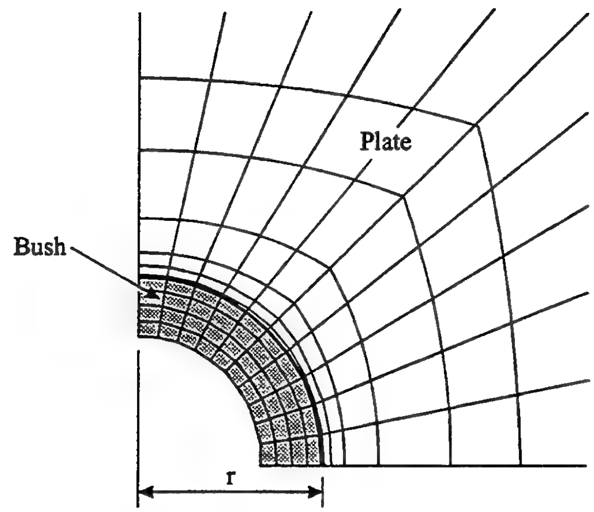

(b) Region near hole/bush interface

Figure 2. Typical finite-element mesh for interference-fit bush in a plate

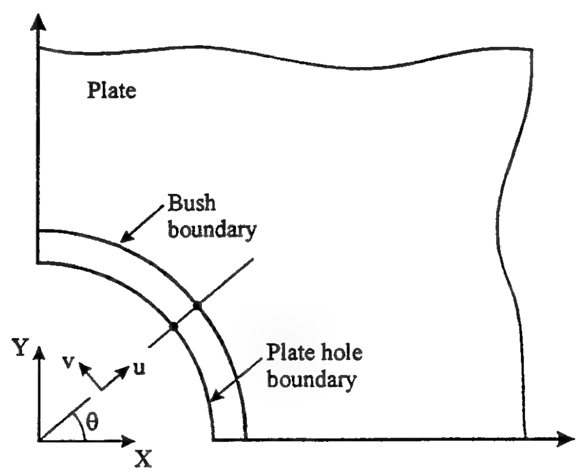

Figure 3. Generic geometry for definition of interference-fit boundary conditions along bush/plate interface prior to bush insertion

2.2 Comparison with Published Results for Plate Stresses

Two benchmark FE analyses were undertaken to gain confidence in the FE modelling method used for simulating slip and no-slip conditions; one to compare with the no-slip study of an interference-fit bush in a plate [1], and the other to compare with Crews' analysis of an interference-fit bolt in a plate for the condition of full-slip [3]. In these reference cases stresses in the plate were determined with and without a remote load applied.

2.2.1 Plate with Interference-Fit Bush for No-Slip Condition

To enable comparison with Piperias and Heller [1] the plate and bush were assigned the properties of aluminium alloy; with $E_{plate}/E_{bush} = 1$, $\nu = 0.33$, the ratio of bush thickness to hole radius (t/r) was 0.336, and the bush radial interference level was 1.0% of the hole radius.

The model consisted of 175 isoparametric rectangular elements with the no-slip constraint applied to the plate/bush interface. For the two locations considered in the plate, ie, 0° and 90° around the hole, the values of interference stress and alternating stress concur within 2% of those presented in [1]. The very small discrepancy in results is believed to be due to the difference in the size of the plate modelled; a width and height of 15r and 30r respectively, as compared to 20r and 40r respectively as used in [1]; and numerical error.

2.2.2 Plate with Interference-Fit Plug for Slip Condition

The problem of an interference-fit plug (full bush) for the condition of frictionless contact between the plug and plate is compared to a numerical analysis given by Crews [3]. For this analysis the plate and bush were aluminium alloy; with $E_{plate}/E_{bush} = 1$, $\nu = 0.33$, and the bush radial interference level was 1.0% of the hole radius.

The model consisted of 195 isoparametric rectangular elements. The values of interference and total stresses in the plate around the hole concurred within 2.5% of those presented in [3] for the corresponding case. Again, the discrepancy in results could be attributed to the difference in the size of the plate modelled; a width and height of 15r and 30r respectively, as compared to an infinite plate as used in [3]; and numerical error.

2.3 Numerical Analysis of Various Modulus Interference-Fit Bushes

From the satisfactory results of the two benchmark problems, it was thus assumed that the plate/bush system was sufficiently well modelled. The geometric modelling details as described in Section 2.1 above were used for the numerical stress analysis of the interference-fit bushes. Four different types of bush material were analysed;

namely (i) polycrystalline alumina, (ii) mild steel, (iii) aluminium and (iv) tungsten-carbide. The bushes had a wall thickness of 3.36 mm, resulting in a bush thickness to hole radius ratio of 0.336—the same as that for the tested specimens (where t/r = 2.02/6.01) described in Section 3. As mentioned above, the plate was aluminium alloy and both no-slip and full-slip cases were studied. The resultant FE mesh was the same for both cases and consisted of 175 eight-noded isoparametric elements; 135 plate elements and 40 bush elements. Table 1 summarizes the stresses and strains in the bush due to an interference-fit only of 0.5% (based on hole radius) for the no-slip and slip cases, and also lists the appropriate material properties, E and ν, for each bush. Results are presented at four locations on the bush; namely points A and B located on the bush/plate interface on the X-axis and Y-axis respectively, and points C and D located on the inner surface of the bush on the Y-axis and X-axis respectively; as shown in Figure 4. It should be noted that stresses due to interference only are linear, thus the stress values at different interference levels can be readily determined through linear scaling.

The alternating radial and hoop stresses in the bush due to an applied remote load are presented in Table 2 for each of the different bush materials. These results, which are for the conditions of no-slip and slip between the bush and plate for locations A-D, have been normalized with respect to the remote applied stress, and are valid for an applied stress less than or equal to the separation stress (σ_{sep}) listed. The separation stress is defined as the remote load required to cause separation between a pair of nodes on the bush/plate boundary. It is equivalent to the radial stress at the hole being zero at that location.

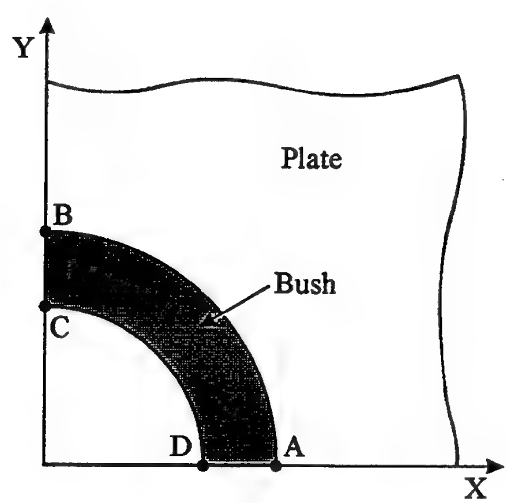

Figure 4. Locations A-D on bush

Table 1. Bush stresses and strains at selected locations due to 0.5% interference fit only in an aluminium plate

Bush material	Case	Location	Stress (MPa) Radial	Stress (MPa) Hoop	Stress (MPa) von Mises	Strain (με) Radial	Strain (με) Hoop
Tungsten-carbide	No slip	A	-214.2	-560.0	489.4	-158.1	-945.8
E = 540 GPa		B	-214.3	-564.1	493.2	-156.5	-953.4
ν = 0.23		C	-2.99	-762.6	761.1	319.3	-1411
		D	-3.25	-789.5	787.9	330.3	-1461
	Slip	A	-213.2	-549.9	480.2	-160.6	-927.5
		B	-215.2	-574.1	502.3	-152.0	-971.4
		C	-2.94	-758.9	757.4	317.8	-1404
		D	-3.30	-793.3	791.6	331.8	-1468
Alumina	No slip	A	-199.7	-523.1	457.2	-196.7	-1221
E = 390 GPa		B	-199.6	-524.4	458.4	-195.7	-1224
ν = 0.235		C	-2.82	-712.5	711.1	422.1	-1825
		D	-3.03	-733.7	732.2	434.3	-1879
	Slip	A	-198.9	-514.7	449.6	-199.7	-1200
		B	-200.3	-532.6	466.0	-192.7	-1245
		C	-2.79	-710.4	709.0	420.9	-1820
		D	-3.06	735.9	734.4	435.6	-1885
Steel	No slip	A	-166.4	-436.8	381.8	-169.0	-1851
E = 209 GPa		B	-166.1	-435.2	380.4	-169.9	-1844
ν = 0.3		C	-2.59	-595.8	594.5	842.8	-2847
		D	-2.72	-608.4	607.0	860.3	-2907
	Slip	A	-165.8	-431.4	376.9	-174.2	-1826
		B	-166.6	-440.5	385.3	-164.7	-1869
		C	-2.58	-595.6	594.3	842.6	-2846
		D	-2.73	-608.6	607.3	860.5	-2908
Aluminium	No slip	A	-98.45	-258.7	226.2	-180.6	-3125
E = 72.4 GPa		B	-98.27	-257.2	224.8	-184.9	-3105
ν = 0.33		C	-1.62	-354.3	353.5	1592	-4886
		D	-1.66	-358.2	357.4	1610	-4941
	Slip	A	-98.27	-256.9	224.5	-186.3	-3100
		B	-98.45	-259.0	226.4	-179.3	-3129
		C	-1.63	-354.8	354.0	1595	-4893
		D	-1.66	-357.8	356.9	1608	-4934

The FE analysis shows that the interference stresses and strains for the no-slip and slip cases are similar. The small difference between them is due to the (non-infinite) geometry of the plate rendering the problem non-axi-symmetric. Less constraint was provided by the finite width than by the height. Numerical error is the reason for the radial stresses at the inner locations (C and D) not being equal to zero. The results also indicate that the magnitude of the bush stresses decreases with decrease in stiffness as expected, ie, the stiffer the bush material the more stress it can carry. The magnitude of the strains increase as stiffness decreases, showing that the less stiff the bush, the more it deforms. The inside surface of the bush experiences a larger magnitude of hoopwise stress and strain than the bush/plate interface. The FE analysis shows that the alumina bush had to endure tensile strains; which it could not. This, along with

the three-dimensional stress field arising during insertion, was the reason why the alumina failed.

Table 2. Bush normalized alternating stresses at selected locations

Bush material	Case	Location	Normalized alternating stress Radial	Hoop
Tungsten-carbide	**No slip**	**A**	0.583	0.730
		B	0.618	2.420
σ_{sep} = 204 MPa		**C**	-0.052	-4.067
		D	0.069	8.416
	Slip	**A**	0.139	-4.066
		B	1.053	7.193
		C	-0.074	-5.853
		D	0.092	10.18
Alumina	**No slip**	**A**	0.590	1.235
σ_{sep} = 218 MPa		**B**	0.528	1.698
		C	-0.043	-3.258
		D	0.059	7.308
	Slip	**A**	0.190	-3.026
		B	0.919	5.937
		C	-0.058	-4.368
		D	0.074	8.394
Steel	**No slip**	**A**	0.553	1.751
σ_{sep} = 242 MPa		**B**	0.377	0.688
		C	-0.032	-2.089
		D	0.047	5.457
	Slip	**A**	0.234	-1.529
		B	0.689	3.950
		C	-0.036	-2.226
		D	0.051	5.575
Aluminium	**No slip**	**A**	0.371	1.517
σ_{sep} = 272 MPa		**B**	0.178	-0.079
		C	-0.017	-1.020
		D	0.027	3.007
	Slip	**A**	0.183	-0.346
		B	0.362	1.776
		C	-0.013	-0.520
		D	0.022	2.499

The data of Table 2 show that the addition of a remote stress results in a difference between the no-slip and slip values of normalized alternating stress, especially on the bush/plate interface. A marked variation in the bush stresses between the 0° and 90° locations, especially the hoop stresses, which are greater for the higher modulus bushes, and on the inside surface of the bush, is indicated. Again, the radial values at locations C and D should be zero. As for the hoop stresses, the radial stresses tend to be higher for the stiffer material. The separation stress is shown to increase with a decrease in bush stiffness indicating, as previously, that the less stiff the bush, the more it deforms.

3. Experimental Analysis of Thick-Walled Bush Specimens

As mentioned in Section 1, preliminary tests were undertaken with specimens similar to those described in Section 3.1 below. These tests highlighted the ability of the interference-fit bush to reduce the stress concentration in the plate. The stress concentration of the hole was reduced such that failure in the fillet region was common. The fillets were therefore altered, however then failure tended to be initiated from the surface of the test section. The test section of the preliminary specimens was polished with distilled water or kerosene as the lubricant, however, this did not help prevent surface cracks from forming in this region. A 1990 report on this topic [6] concluded that the surface cracks in 7050 aluminium alloy specimens "had initiated from corrosion pitting and intergranular cracking associated with the corrosion pitting", and "that the corrosion took place during and/or after the polishing phase of specimen preparation". These preliminary tests concluded that surface treatments (of rounding and polishing the edges, and shot-peening) of the fillets, were necessary to transfer failure to the test section, and that polishing of the test section of the plate may be detrimental. Hence for the present tests, the specimens had (i) modified fillets (where necessary) and (ii) an unpolished test section.

3.1 Specimen Details

The specimens were comprised of two components; namely a dog-bone-shaped plate with a central hole, and an interference fit bush; as shown in Figure 5. The dog-bone plate was manufactured from a 144.17 mm thick rolled plate of 7050-T73651 aluminium alloy, the loading direction being the longitudinal direction of the plate. A central pilot hole was drilled and then lightly reamed out to 12.02 mm diameter in the 12.5 mm thick specimen. To increase the probability of failure within the test section, the sharp edges of the fillets were rounded with a file and then polished with 120, 240 and 1200 grit emery paper. The plate (excluding the gripping sections and the test section) was then shot-peened with filtered glass beads at 60 psi (413.7 kPa). The test section of the plate was left unpolished—removal of the machining marks was believed to perhaps remove beneficial residual surface compressive stresses

The interference-fit bushes were manufactured from aluminium alloy 7050-T73651, stainless steel (type 304) or tungsten-carbide (grade H15F) and were precisely ground to produce an interference fit of 0.5% with the holes of the dog-bone plates (ie, elastic deformation of the aluminium plate). The actual values of interference for each specimen are listed in Table 3 and range from 0.50 to 0.51%. The wall thickness of the bushes was 2 mm, which gave the same relative wall thickness as analysed in Section 2.3. Both the plate and bush were degreased prior to assembly. The shallow taper on the outside surface of the bush allowed easy alignment with the plate hole. The bush, which was lubricated with barium chromate, was then inserted using a standard servohydraulic test machine.

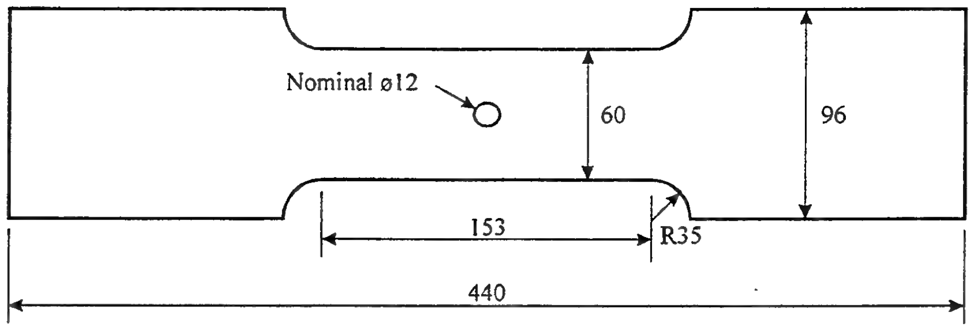

(a) plate

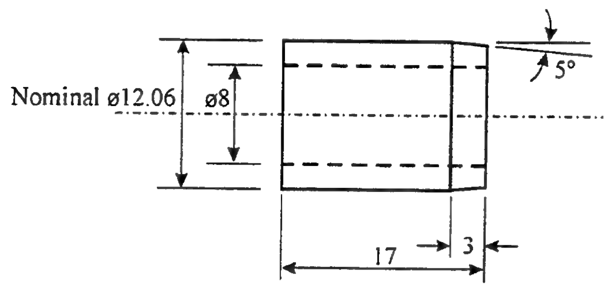

(b) bush

Figure 5. Geometry of interference-fit thick-walled bush specimens

Table 3. Plate and thick-walled bush combinations and resultant interference-fit levels

Specimen	Hole Dia. (mm)	Bush	Outer Dia. (mm)	Interference (%)
		Tungsten-carbide		
KD1S17	12.020	WC-20	12.081	0.51
KD1S4	12.020	WC-16	12.081	0.51
KD1S10	12.020	WC-18	12.081	0.51
		Steel		
KD1S3	12.019	ST-3	12.080	0.51
KD1S8	12.019	ST-6	12.080	0.51
KD1S23	12.019	ST-7	12.080	0.51
		Aluminium		
KD1S15	12.018	AL-3	12.078	0.50
KD1S11	12.018	AL-8	12.079	0.51
KD1S9	12.019	AL-2	12.079	0.50
		Hole Only		
KD1S2	12.011			
KD1S29	12.020			
KD1S24	12.020			

3.2 Testing Details

The fatigue tests were conducted in an Instron 250 kN test machine with PC interface to specify and monitor the load sequence applied. The load sequence utilized was of a flight-by-flight type developed from the stress history of the wing root of an Australian F/A-18 aircraft. Each repeated loading block (program) was equivalent to 302.9 flight hours and consisted of 22,010 turning points, with a minimum stress of $-0.38\sigma_{max}$. The average cyclic frequency used was 10 Hz. Testing was conducted at a maximum net-stress level of 200 MPa, based on the minimum cross-sectional area of the plate. A total of 12 tests were performed and consisted of three of each of the following specimen types:

(i) plate with tungsten-carbide interference-fit bush,
(ii) plate with steel interference-fit bush,
(iii) plate with aluminium interference-fit bush, and
(iv) plate with open hole.

The stress concentration factor due to remote loading (K_t) for each specimen type is 0.28, 0.74, 1.53 and 3.07 respectively, as determined from the no-slip FE analysis.

3.3 Results and Discussion

The fatigue lives of the specimens are listed in Table 4 in flight hours and the relative mean lives are given in Table 5. The results show that the increase in life of all of the bushed specimens over the hole-only specimens was very large (at least 10.9 times). It also appears that the longer fatigue lives are associated with the low modulus bushes. Thus, it appears that effects not accounted for in theory [1-4] dominated.

Table 4. Spectrum fatigue lives of thick-walled bush modulus specimens

Bush	Life (flight hours)	Log. average fatigue life (flight hours)
Tungsten-carbide	152346	
	167388	162834
	169308	
Steel	88926	
	393757	215270
	284902	
Aluminium	226442*	
	415561	431313
	447663	
Hole only	13794	
	14545	14948
	16647	

* from surface, thus disregarded

Table 5. Ratios of average lives of thick-walled bush modulus specimens

Comparison	Ratio of mean lives
Tungsten – carbide bush / Hole only	10.89
Steel bush / Hole only	14.40
Aluminium bush / Hole only	28.85

The thick-bushed specimens had lives which were similar to that of a plate without a hole. The interference-fit 2 mm thick bushes significantly reduced the K_t of the hole such that surface treatments were necessary to reduce the chance of failure in the fillet region or surface of the plate. The high modulus bushed specimens experienced an increased mean stress level. This may have contributed to their shorter lives.

A similar degree of fretting was apparent on all bushed specimens, however, the fretting of the steel bushed specimens tended to be more concentrated. The aluminium and steel bushes also showed fretting wear; the fretting of the tungsten-carbide bushes was comparatively small. Typical fracture surfaces are given in Figure 6. With the bushed specimens, the crack origins appear to be subsurface, from voids or inclusions adjacent to the hole. Under a microscope, a small 45° lip adjacent to the hole of the tungsten-carbide and steel bushed specimens was detected. This lip could well be due to Stage I cracking before the crack surface levels out (Stage II). The location of the crack origin and the shape of the elliptical crack surfaces, indicates that the stresses down the bore of the hole are less than those due to adjacent subsurface inclusions. Figure 6 also shows that the 7050 aluminium alloy has a coarse grain size.

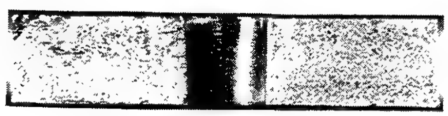

(a) aluminium bushed specimen

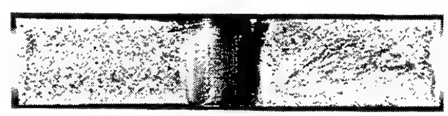

(b) steel bushed specimen

(c) tungsten-carbide bushed specimen

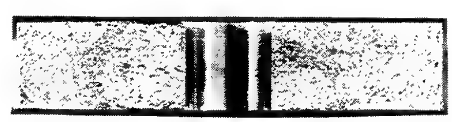

(d) hole only specimen

Figure 6. Specimen fractures of 7050 alloy plate (actual width of fracture plane is 60 mm)

The results clearly indicated that there is no benefit in reducing the K_t of the hole in the plate to significantly less than one. Due to these interesting results, it was decided to repeat these tests with values of K_t close to or greater than one by using thin-walled bushes as described below.

4. Experimental Analysis of Thin-Walled Bush Specimens

4.1 Specimen Details

The thin-walled bush specimens were very similar to those described in Section 3.1, as shown in Figure 7. The plate geometry was only slightly different, ie, in the fillet region and length, as compared to the previous specimens. However, the key difference was that the bush wall thickness was reduced from 2 mm to 1 mm.

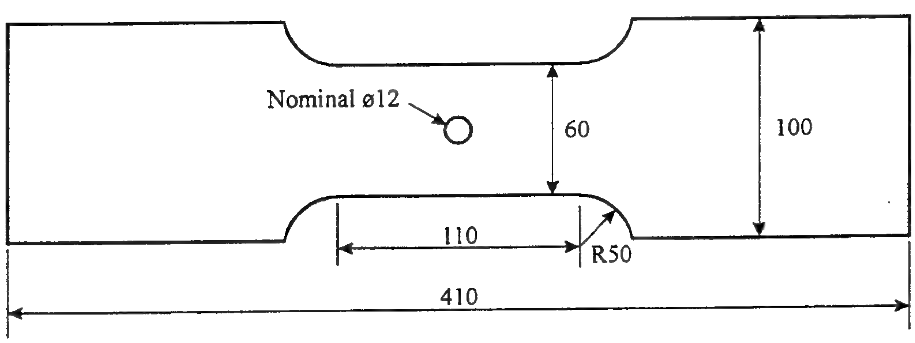

(a) plate

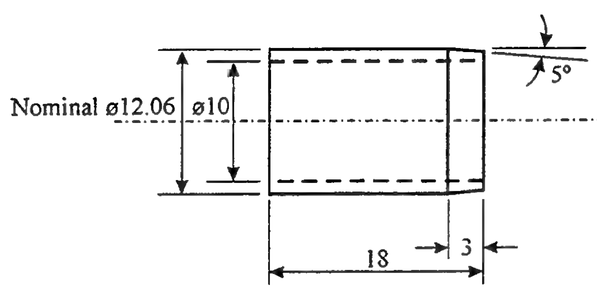

(b) bush

Figure 7. Geometry of interference-fit thin-walled bush specimens

The dog-bone plate was manufactured from a 2530 mm length extruded bar of 7075-T73511 aluminium alloy with a rectangular cross-section of 127 mm x 76.2 mm, the loading direction being the longitudinal direction of the bar. To increase the probability of failure within the test section, the sharp edges of the steel and tungsten-carbide bushed specimen fillets' were rounded with a file and then polished with 120, 240 and 1200 grit emery paper. The plate for the tungsten-carbide bushed specimens (excluding the gripping sections and the test section) were also shot-peened with filtered glass beads at 60 psi (413.7 kPa).

The interference-fit bushes, which had a wall thickness of 1 mm, were manufactured from aluminium alloy 7075 (DTD 683), stainless steel (type 304) or tungsten-carbide (grade H15F). They were ground to produce an interference fit of 0.5% with the holes of the dog-bone plates (ie, elastic deformation of the aluminium plate). The actual values of interference for each specimen are listed in Table 6 and range from 0.52 to 0.55%.

Table 6. Plate and thin-walled bush combinations and resultant interference-fit levels

Specimen	Hole Dia. (mm)	Bush	Outer Dia. (mm)	Interference (%)
		Tungsten-carbide		
KG2D4	12.014	WC-D1	12.079	0.54
KG2C2	12.013	WC-C4	12.077	0.53
KG2G4	12.014	WC-D4	12.078	0.53
KG2D3	12.012	WC-D3	12.075	0.52
		Steel		
KG2B2	12.015	ST-B4	12.079	0.53
KG2B3	12.016	ST-B2	12.080	0.53
KG2E4	12.013	ST-C2	12.078	0.54
KG2C3	12.017	ST-B1	12.081	0.53
		Aluminium		
KG2F2	12.015	AL-E2	12.081	0.55
KG2C4	12.013	AL-E1	12.077	0.53
KG2F3	12.014	AL-F2	12.078	0.53
KG2E3	12.013	AL-F1	12.077	0.53
		Hole Only		
KG2C1	12.014			
KG2D1	12.014			
KG2G1	12.012			
KG2G3	12.013			

4.2 Testing Details

The specimens were tested in the same manner as the thick-walled bush specimens except the net-area stress was increased to 280 MPa, and four of each of the specimen types (as listed in Section 3.2) were tested. The K_t due to remote loading for each of the thin-walled bush specimen types is 0.74, 1.35, 2.10 and 3.07 respectively, as determined from the no-slip FE analysis.

4.3 Results and Discussion

The fatigue lives of the specimens are listed in Table 7 in flight hours and the relative mean lives are given in Table 8. The results show that, on average, the higher the modulus of the interference-fit bush, the longer the life of the specimen.

Table 7. Spectrum fatigue lives of thin-walled bush modulus specimens

Bush	Life (flight hours)	Log. average fatigue life (flight hours)
Tungsten-carbide	39140	
	32410	45367
	81341	
	41055	
Steel	37565	
	33022	37393
	33785	
	46652	
Aluminium	26438	
	20300	24949
	26170	
	27587	
Hole only	5742	
	6537	5865
	5920	
	5325	

Table 8. Ratios of average lives of thin-walled bush modulus specimens

Comparison	Ratio of mean lives
$\frac{\text{Tungsten – carbide bush}}{\text{Hole only}}$	7.74
$\frac{\text{Steel bush}}{\text{Hole only}}$	6.38
$\frac{\text{Aluminium bush}}{\text{Hole only}}$	4.25

As mentioned previously, the interference-fit 1 mm thick tungsten-carbide and steel bushes reduced the K_t of the plate hole to a value of 0.74 and 1.35 respectively, and to 2.10 for the aluminium bushed specimens. On average, the steel and tungsten-carbide bushed specimens had a longer life than the aluminium bushed specimens. However, as the value of K_t for these higher modulus bushed specimens was around one, the increase in life over the aluminium bushed specimens was not substantial.

A similar degree of fretting was apparent on all bushed specimens and bushes. Typical fracture surfaces are shown in Figure 8. It can be assumed that fretting did not dominate due to the relative shortness of the specimen lives. With the bushed specimens, the crack origins appear to be on the free surface of the plate adjacent to the hole. This, and the elliptical crack shape, indicates that the stresses on the free surface are greater than those down the bore of the hole. Figure 8 shows that the 7075 aluminium alloy has a much finer grain size than the 7050 alloy.

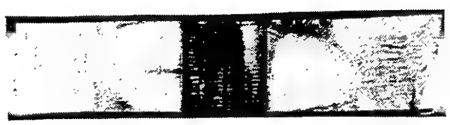

(a) aluminium bushed specimen

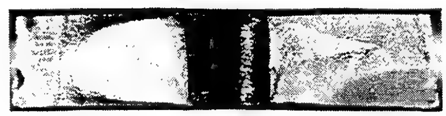

(b) steel bushed specimen

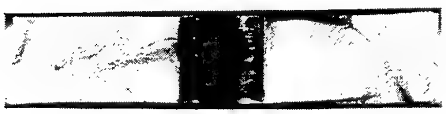

(c) tungsten-carbide bushed specimen

(d) hole only specimen

Figure 8. Specimen fractures of 7075 alloy plate (actual width of fracture plane is 60 mm)

5. Conclusions

In this testing program the fatigue life of plates with central holes, with thick and thin various modulus interference-fit bushes, was determined under a representative fighter-aircraft loading sequence. The test results of the thin-bushed specimens indicated that the higher the modulus of the interference-fit bush, the longer the fatigue life of the specimen. On average, the steel and tungsten-carbide bushed specimens had a longer life than the aluminium bushed specimens. However, as the stress concentration factor (due to remote loading) for these higher modulus bushed specimens was around one, the increase in life over the aluminium bushed specimens was not substantial. The thick-wall bushed specimens experienced an increase in life of between 10.9 and 28.9 times the life of the hole-only specimens, where the longer lives appeared to be associated with the low modulus bushes. The high modulus bushed specimens experienced an increased mean stress level. This may have contributed to their shorter lives.

The results of the testing program clearly showed that there is no benefit in reducing the stress concentration factor (due to remote loading) of the hole in the plate to less than one. Depending on the relative thickness and modulus of the interference-fit bush, different failure modes can result. Thus, in practice, the higher the relative bush modulus does not necessarily correspond to a better solution for life extension (compared to that of a lower modulus bush).

The finite element work conducted determined stresses and strains in interference-fit bushes of different materials. Conditions of no-slip and full-slip between the bush and plate were modelled. The finite-element analyses showed that the maximum stress in the bush increased with increase in bush modulus. It was also found that high tensile strains occurred in the bush at the inner surface. It is believed that these tensile strains may have been the reason why the alumina bushes used in preliminary tests failed on insertion.

6. Acknowledgements

Dr M Heller's and Dr JM Finney's guidance and contributions towards this report were greatly appreciated. The author also wishes to thank the fatigue testing laboratory staff who worked on this testing program and Mr NT Goldsmith for his fractographic advice.

7. References

1. P Piperias & M Heller, "Optimisation of stresses around holes using sleeve/bolt combinations", 1993, *Proceedings of the 5th Australian Aeronautical Conference, Melbourne* pp 309-315.

2. B Koplik & DD Klassen, "Reduction of alternating stress range around holes in flat plates by use of inserts", 1971, *Journal of Engineering for Industry* pp 683-687.

3. JH Crews, "An elastic analysis of stresses in a uniaxially loaded sheet containing an interference-fit bolt", 1972, NASA TN D-6955.

4. GS Jost, "Stresses and strains in plain and coldworked annuli subjected to remote, interference or combined loading", 1992, ARL Structures Report 446.

5. RB Allan & M Heller, "Elastic-plastic stress analysis of a plate containing a round hole with combined cold expansion and interference fitting under F-111C representative loading conditions", AMRL Research Report in publication, File No. M1/9/167.

6. SA Barter, "Examination of crack initiation points in 7050 fatigue specimen", 15/6/90, ARL Letter Report No. M2/90.

DISTRIBUTION LIST

Effectiveness of high modulus interference-fit bushes for fatigue life extension of plates with circular holes

Rebecca Evans

AUSTRALIA

1. DEFENCE ORGANISATION

a. Task Sponsor AIR OIC ASI-LSA

b. S&T Program

Chief Defence Scientist
FAS Science Policy
AS Science Industry and External Relations
AS Science Corporate Management
} shared copy

Counsellor Defence Science, London (Doc Data Sheet)
Counsellor Defence Science, Washington (Doc Data Sheet)
Scientific Adviser to MRDC Thailand (Doc Data Sheet)
Director General Scientific Advisers and Trials/Scientific Adviser Policy and Command (shared copy)
Navy Scientific Adviser (3 copies Doc Data Sheet and 1 copy distribution list)
Scientific Adviser - Army (Doc Data Sheet and distribution list only)
Air Force Scientific Adviser
Director Trials

Aeronautical and Maritime Research Laboratory
Director

Electronics and Surveillance Research Laboratory
Director

Chief of Airframes and Engines Division
Research Leader Fracture Mechanics
Research Leader Structural Integrity
Research Leader Structural Dynamics
Research Leader Aerospace Composite Structures
M. Heller (3 copies)
A.D. Graham
K.C. Watters
R.G. Parker
I.A. Anderson
W.B. Madley
R.L. Evans

DSTO Library
Library Fishermens Bend
Library Maribyrnong
Library DSTOS (2 copies)
Australian Archives
Library, MOD, Pyrmont (Doc Data sheet only)

c. **Forces Executive**
Director General Force Development (Sea) (Doc Data Sheet only)
Director General Force Development (Land) (Doc Data Sheet only)
Director General Force Development (Air)

e. **Army**
ABCA Office, G-1-34, Russell Offices, Canberra (4 copies)

f. **Air Force**
CENG, 501 Wing, Amberley

g. **S&I Program**
Defence Intelligence Organisation
Library, Defence Signals Directorate (Doc Data Sheet only)

i. **B&M Program (libraries)**
OIC TRS, Defence Central Library
Officer in Charge, Document Exchange Centre (DEC), 1 copy
*US Defence Technical Information Center, 2 copies
*UK Defence Research Information Centre, 2 copies
*Canada Defence Scientific Information Service, 1 copy
*NZ Defence Information Centre, 1 copy
National Library of Australia, 1 copy

2. **UNIVERSITIES AND COLLEGES**

Australian Defence Force Academy
Library
Head of Aerospace and Mechanical Engineering
Deakin University, Serials Section (M list), Deakin University Library, Geelong, 3217
Senior Librarian, Hargrave Library, Monash University
Librarian, Flinders University

3. **OTHER ORGANISATIONS**

NASA (Canberra)
AGPS
ASTA Engineering, Document Control Office
Hawker de Havilland Aust Pty Ltd, Bankstown, Library
BHP Melbourne Research Laboratories

OUTSIDE AUSTRALIA

4. **ABSTRACTING AND INFORMATION ORGANISATIONS**
   INSPEC: Acquisitions Section Institution of Electrical Engineers
   Library, Chemical Abstracts Reference Service
   Engineering Societies Library, US
   Materials Information, Cambridge Scientific Abstracts, US
   Documents Librarian, The Center for Research Libraries, US

5. **INFORMATION EXCHANGE AGREEMENT PARTNERS**
   Acquisitions Unit, Science Reference and Information Service, UK
   Library - Exchange Desk, National Institute of Standards and Technology, US
   National Aerospace Laboratory, Japan
   National Aerospace Laboratory, Netherlands

SPARES (10 copies)

Total number of copies: 76

DEFENCE SCIENCE AND TECHNOLOGY ORGANISATION
DOCUMENT CONTROL DATA

1. PRIVACY MARKING/CAVEAT (OF DOCUMENT)

2. TITLE Effectiveness of High Modulus Interference-Fit Bushes for Fatigue Life Extension of Plates with Circular Holes	3. SECURITY CLASSIFICATION (FOR UNCLASSIFIED REPORTS THAT ARE LIMITED RELEASE USE (L) NEXT TO DOCUMENT CLASSIFICATION) Document (U) Title (U) Abstract (U)
4. AUTHOR(S) Rebecca Evans	5. CORPORATE AUTHOR Aeronautical and Maritime Research Laboratory PO Box 4331 Melbourne Vic 3001

6a. DSTO NUMBER	6b. AR NUMBER	6c. TYPE OF REPORT	7. DOCUMENT DATE
DSTO-TR-0477	AR-010-105	Technical Report	February 1997

8. FILE NUMBER	9. TASK NUMBER	10. TASK SPONSOR	11. NO. OF PAGES	12. NO. OF REFERENCES
M1/9/185	95/228	AIR	18	6

13. DOWNGRADING/DELIMITING INSTRUCTIONS	14. RELEASE AUTHORITY
None	Chief, Airframes and Engines Division

15. SECONDARY RELEASE STATEMENT OF THIS DOCUMENT

Approved for public release

OVERSEAS ENQUIRIES OUTSIDE STATED LIMITATIONS SHOULD BE REFERRED THROUGH DOCUMENT EXCHANGE CENTRE, DIS NETWORK OFFICE, DEPT OF DEFENCE, CAMPBELL PARK OFFICES, CANBERRA ACT 2600

16. DELIBERATE ANNOUNCEMENT

No limitations

17. CASUAL ANNOUNCEMENT Yes

18. DEFTEST DESCRIPTORS

Fatigue life; Interference fit devices; Sleeves; Holes; Plates

19. ABSTRACT
An experimental program has been carried out to examine the influence of bush modulus on the fatigue lives of aluminium alloy specimens with bushed holes of 12 mm diameter. The specimens, with 1 mm or 2 mm thick bushes of 0.5% interference fit and of widely different modulus, were fatigue tested under a representative fighter-aircraft loading sequence. The thin-walled bushes were found to extend the fatigue lives of the plates with holes by at least 4.2 times, and the thick-walled bushes produced at least a 10.9 times increase in life. The test results also indicated that different failure modes can occur depending on the relative thickness and modulus of the interference-fit bush. Thus, the specimens with the highest bush modulus did not necessarily have the longest lives, even though the stress concentration factor (due to remote loading) at the hole edge for these specimens was the lowest. Finite-element work was also conducted to determine the stresses and strains in the interference-fit bushes for conditions of no-slip and frictionless contact between the bush and plate. High tensile strains were found to occur in the bush at the inner surface.